The Proton Storage Ring: problems and solutions

R. J. Macek
Los Alamos National Laboratory
Los Alamos, NM 87545
USA

ABSTRACT: The Los Alamos Proton Storage Ring (PSR) now operates with 35μA at 20-Hz pulse repetition rate. Beam availability during 1988 suffered because of a number of problems with hardware reliability and from narrow operating margins for beam spill in the extraction line. A strong effort is underway to improve reliability with an eventual goal of obtaining beam availability in excess of 75%. Beam losses and the resulting component activation have limited operating currents to their present values. In detailed studies of the problem, loss rates were found to be approximately proportional to the circulating current and can be understood by a detailed accounting of emittance growth in the two-step injection process along with Coulomb scattering of the stored beam during multiple traversals of the injection foil. It is now apparent that the key to reducing losses is in reducing the number of foil traversals. A program of upgrades to reduce losses and improve the operating current is being planned.

1. Introduction

The Proton Storage Ring (PSR) at Los Alamos functions as a high-current accumulator or pulse compressor to provide intense pulses of 800-MeV protons for the Los Alamos Neutron Scattering Center (LANSCE) spallation Neutron Source. The neutron scattering community has seen several proposals for similar neutron sources based on compressor rings fed from a proton linac e.g., SNQ from Jülich, one from Moscow, JHP from Japan, and LANSCE II from Los Alamos. To date, only the PSR has been constructed, hence

the experience with PSR should be helpful in assessing this approach to the design of advanced neutron sources.

1.1 Layout

The layout of PSR in relationship to other relevant facilities at the LAMPF site is shown schematically but not to scale in Fig. 1. An 800-MeV H^- beam from the LAMPF linac is kicked into Line D and transported through Line D and the Ring Injection Line to a high-field stripper magnet where it is converted with 100% efficiency to H^o. The H^o beam then enters the lattice of the ring through a dipole and is stripped to H^+ beam with $\sim$ 92% efficiency in a 200 g/cm^2 carbon foil. Up to 2800 turns can be injected and accumulated during a single macropulse. Beam is normally extracted in a single turn shortly after the end of injection and transported to the LANSCE neutron-production target in ER-1.

1.2. Performance to Date

Performance parameters of general interest are summarized in Table I where the values as of October 1988 are compared with the design goals. The peak current (on the 100 nanosecond time scale) available from LAMPF is 8-10 mA and is limited by the H^- source. By increasing the pulse length beyond the design value to 950 μS we have accumulated (in test runs) as many as 3.8 x 10^{13} protons per pulse (ppp) or 70% of the original design goal for this parameter. Unfortunately, we cannot use this peak intensity for routine operation because of "slow" losses during accumulation. In the present operation at 20 Hz, we are limited to an average current of 35μA by losses of $\sim$ 0.5 A which have caused activation at the maximum acceptable level for hands-on maintenance of ring components. These losses occur primarily in the injection and extraction regions which contain the known limiting apertures. Further information on the design and initial performance are published elsewhere.[1]

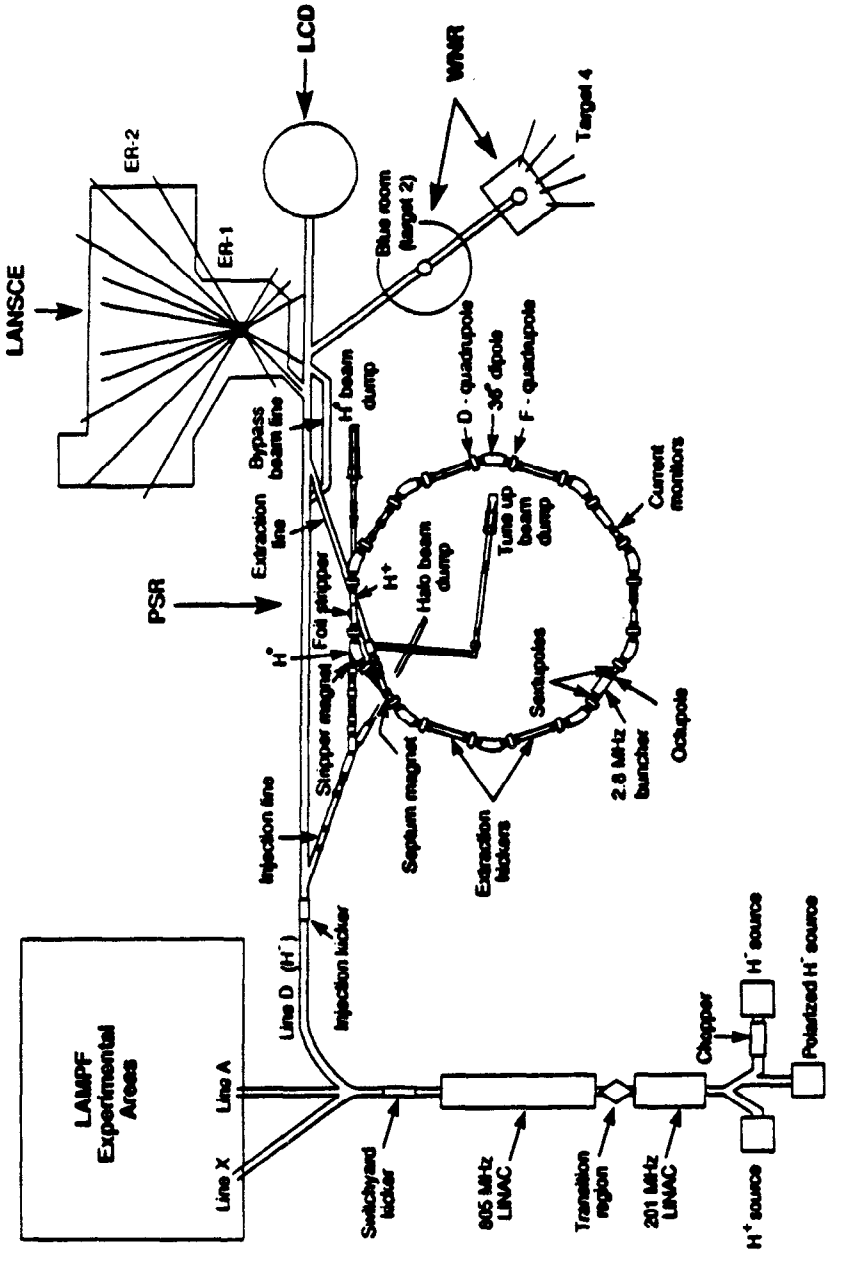

Fig. 1. Schematic layout of PSR at the LAMPF site.

TABLE I. Summary of Performance (to October 1988)

	Design	Achieved	
• Peak Injected Current	15 mA	8-10 mA	
• Injection Pulse Length	750 μs	975 μs	
• Protons/Pulse	5.2×10^{13}	3.8×10^{13}	
• Repetition Rate	12 Hz	20 Hz	
• Average Current	100 μA	35 μA	
• Losses:			
Accumulation	0.1–0.3μA @ 100μA	0.5 μA @ 35 μA	
	[0.1–0.3%]	[1.4%]	
Extraction	<0.1%	0.1–0.3% (@ 30 μA)	
• Availability	75% ?	62% ave. (80% Best Run)	1987
		30% Avg	Cycle 51
		64% Avg	Cycle 52

2. Reliability and Beam Availability

Beam availability was never specified in the original PSR design documents; however, the LANSCE user community has shown a strong preference for a value of 75%, or greater. We define beam availability as the ratio of the time beam was available (at greater than 50% of the scheduled current) for delivery at the LANSCE target to the beam time scheduled for LANSCE research.

2.1. Daily Availability in 1988

The operation of PSR during the summer of 1988 (LAMPF Cycles 51 and 52) was the first attempt at sustained running for a formal users program. Beam availability and machine reliability were a great disappointment especially in Cycle 51 when beam availability was about 30%. The details on a daily basis are shown in Fig. 2 where the availability is plotted as a function of time using only the days when beam was scheduled for research at LANSCE. At the 30% level of reliability, the research program at LANSCE suf-

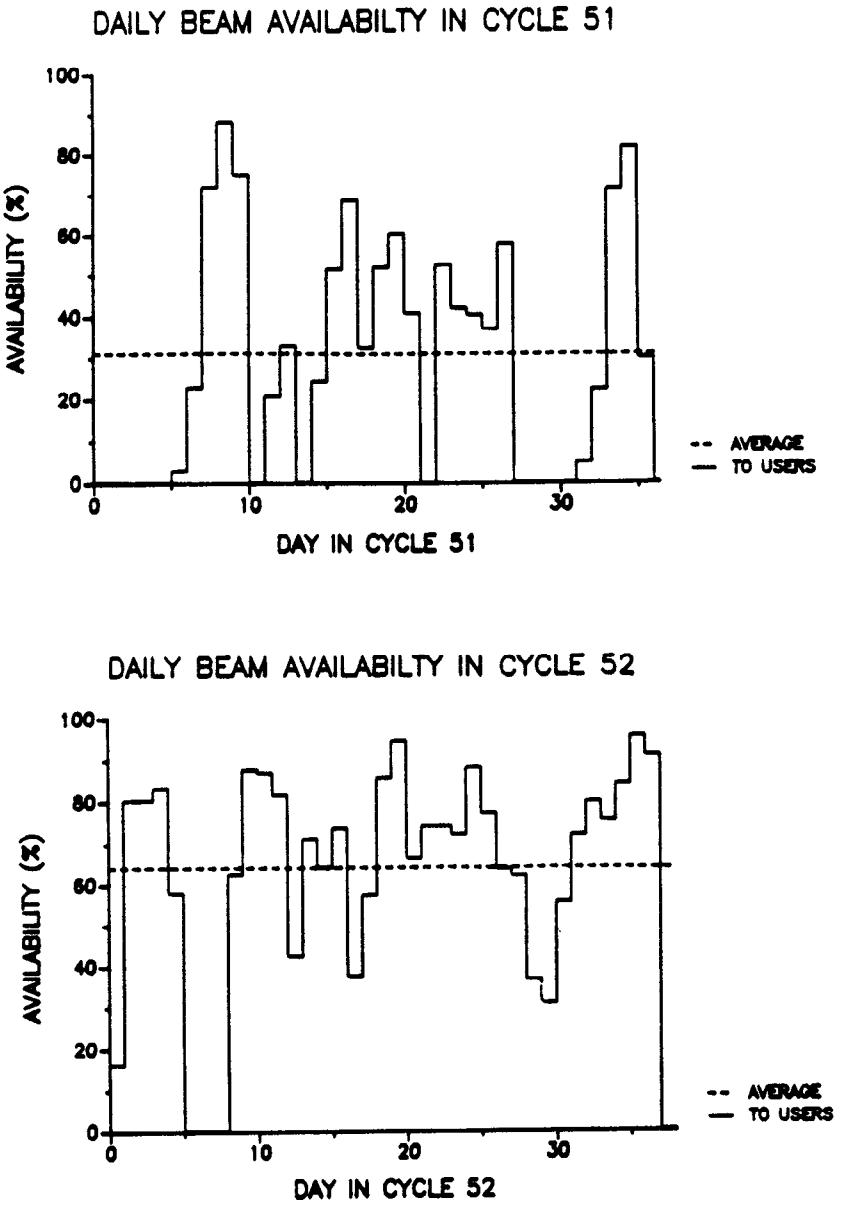

Fig. 2. Daily beam availability in 1988 for LANSCE.

fered; great frustration and dissatisfaction were evident amongst the user community, and the PSR staff became thoroughly exhausted making numerous expedient repairs to more deep-seated problems.

2.2. Subsystems Availability

Much of the downtime came from the pulsed power systems, as can be seen in Table II, Subsystems Availability. Thermal failures of the water-cooled loads on the switchyard kickers and massive failures of high-voltage vacuum feedthroughs on the stripline kickers of the ring extraction system were the most acute of the numerous problems which developed in 1988. Expedient repairs were designed and implemented in the short time between beam cycles in what is best described as a frantic effort to recover the momentum of the LANSCE research program before the end of the 1988 running period. These repairs and a sustained effort to keep all systems operational resulted in a marked improvement in availability which averaged about 65% in cycle 52.

The LAMPF linac is also a significant source of downtime. It is a mature facility whose availability has been 80 to 85% for many years and is at a level that is satisfactory for the nuclear and particle physics program which funds the operation of LAMPF. Further improvement is an expensive undertaking. The 201-MHz RF system is a major source of downtime for the linac and estimates for improving it are between 5 and 10 million dollars; it is not a cost-effective candidate for improving overall reliability. The problem for the LANSCE facility is that beam availability is the product of the availability of LAMPF and that of PSR and the rest of the beam-delivery system. Therefore, to achieve 75% or greater overall availability, the PSR and other beam-delivery system availability will need to reach 95%. This has been achieved with other circular machines such as the Booster Synchrotron at CERN.

2.3. Improvements to Reliability and Operational Efficiency

The H^- source has run at 90 to 95% availability and has required two shifts of downtime every two weeks for reconditioning. Efforts are currently underway to reduce the arc-down rate and improve

Table II. Subsystems Availability in 1988

	Cycle 51	Cycle 52	Long Term Goal
• Linac and H^- Source	75%	82%	85%
• Pulsed Power Systems	68%	94%	
• Other Beam Delivery Systems	85%	91%	95%
Product (Available from PSR)	43%	70%	80%
• Beam On and Current $\geq$ 50% of Scheduled	76%	92%	
• LANSCE Target/Moderator	96%	98%	97%
• Beam Available to Users at $\geq$ 50% of Scheduled Current	31%	64%	>75%

source lifetime. A spare source is being fabricated to reduce the amount of downtime needed for periodic reconditioning. Our goal is source availability of 97-98%.

Many other systems contribute to downtime but a complete discussion is beyond the scope of this paper. The pulsed power systems were discussed earlier. Deionized water systems have presented a number of problems including numerous leaks, corrosion of brass fittings, and deposits in certain power supplies. The use of lead-free solder (95% tin, 5% antimony) with its small workable temperature range undoubtedly contributed to the large number of voids found in the solder joints of the larger copper pipes. Improvements underway include redoing all the joints in the 4-inch water line and more instrumentation to monitor water quality.

Another important loss of beam time arose from frequent tuning to reduce spills in the PSR and in the extraction line. In cycle 51 about 25% of the time when beam otherwise was available, operators were tuning at half or less of the scheduled current primarily to eliminate spills which caused tripping of the errant beam protection instrumentation. Margins on beam spill were much tighter in 1988 than before because users were allowed in the experimental area of LANSCE while beam was on. Prior to 1988 users were excluded when the beam was on. Safe access with the beam on

was guaranteed in 1988 by the newly installed fail-safe Personnel Safety System (PSS) whose three levels of fail-safe errant beam detection instrumentation insured that the beam was promptly shut off under any beam spill conditions which would present a hazard to personnel in occupied areas.

There is very little margin for error in transporting the extracted beam to LANSCE. In the region of transport where the floor of the beam tunnel is also the roof of the experimental area, small spills of order 3-5 nanoamperes (0.01% of the beam) can cause radiation levels of about 20 millirem/hour in certain areas of the experimental hall where users must have free access. In this situation, the least deviation from the optimal tune can cause spills of this magnitude.

The addition of approximately one meter of iron shielding in the extraction channel region over ER-1 would greatly increase the tolerance for error in the beam transport to the LANSCE target. However, the structural modifications needed to support the additional weight are a major complication. Nevertheless, design studies of the changes required for additional shielding of this magnitude are now underway with high priority.

Variations and drifts of the beams, both to and from PSR, can arise from a number of sources including the linac and the beam transport. The beam from the linac changes slightly a few times per shift; these changes are commensurate with our long term experience at LAMPF and can be large enough to have a significant effect at PSR. However, by the end of cycle 52, it became clear that a large portion of the beam changes which affected PSR resulted from poor stability of magnet set points in the Line D transport. A factor of 5 to 10 improvement in magnet-power-supply stability is underway. Longer term, we aim for 0.01% set-point reproducibility, which implies additional improvement in power-supply regulation.

3. Beam Losses[2]

Beam losses during accumulation are far and away the most serious barrier to higher-current operation. In the present operation with 35μA at 20 Hz, the losses produce activation at the limit for hands-

on maintenance of the ring. As we shall demonstrate shortly, the losses at 100μA would be an order of magnitude higher if nothing is done to reduce them.

3.1. General Characteristics of the Accumulation Losses

Slow losses are measured to ~30% accuracy with a series of scintillator-based radiation detectors located on the outside wall of the tunnel at beam height opposite each ring dipole. Detector gains are all identical; signals from each as well as a sum signal of all detectors are used for loss measurements. The sum signal is calibrated by allowing a measured quantity of beam to be completely lost. Fast analog current signals, obtained directly from the phototubes, are available in the control room for detailed analysis of the time structure.

The sum-current signal is a measure of the beam loss rate, $\dot{L}(t)$. A trace from normal operation is shown in Fig. 3 along with a signal from a current monitor that senses the circulating beam current, I(t). The ring current is a ramp because beam is continually injected during an injection period of 375 μs. Fig. 3 shows that $\dot{L}$ is nearly proportional to the stored beam intensity. Total losses, $L = \int \dot{L}\, dt$, will then be quadratic in time. To increase the average current to 100 μA we need to inject for ~1000 μs, but the losses under these conditions are an order of magnitude higher than for the present operation at 375 μs, which already produces the maximum acceptable activation of ring components.

Losses for an extended period of accumulation can arise from those occurring at the time of injection as well as from continual losses of the stored beam. The two components can be separated in an experiment where beam is accumulated for a short time (~100 μs) and stored for a much longer period (~1000 μs) before extraction. Loss rates and circulating current signals from one such experiment for a coasting beam (RF buncher off) are shown in Fig. 4. The discontinuity at the end of injection is caused by the cessation of "first-turn" or injection losses and amounts to ~2 x 10^{-3} of the injected beam current. The loss rate during storage is a slowly increasing function of storage time with a fractional loss rate of ~1.3 x 10^{-5} per proton per turn at the end of the 100-μs injection period.

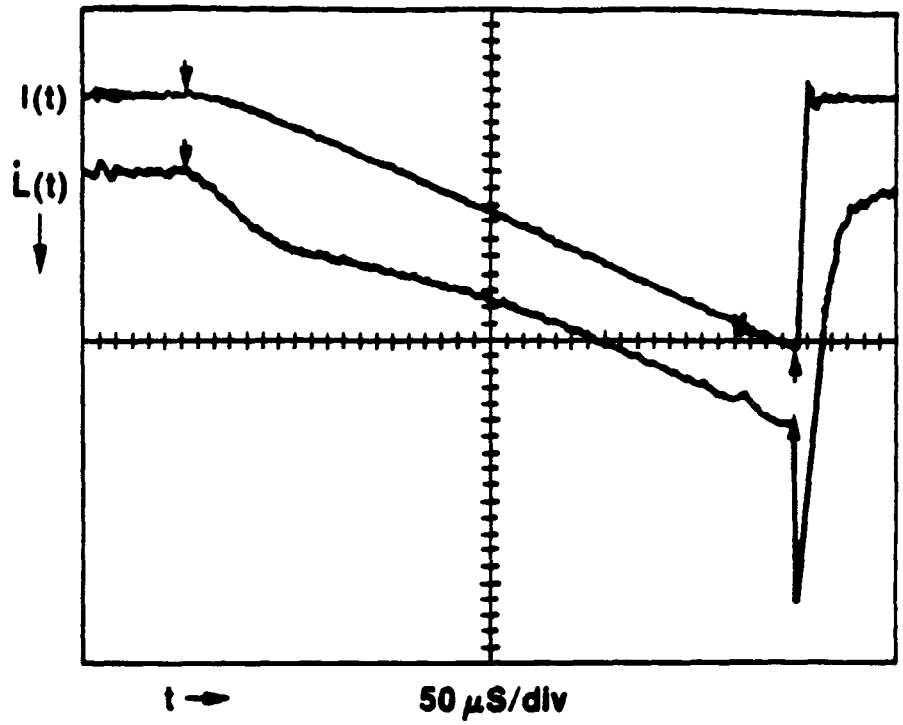

Fig. 3. Loss rate during normal operation.

The significant loss observed during injection and the continual losses thereafter suggest that the injected beam somewhat more than fills the acceptance of PSR. This is corroborated by halo plate scans of the horizontal beam profile in the ring in which a thick plate is scanned across the ring aperture and the fraction of the beam intercepted by the plate is obtained by measuring the scattered beam intensity in the sum of several loss monitors. The signal is normalized to unity when all of the beam is intercepted. This technique is especially useful for measuring the beam distribution in the extremities of the beam. Data from one scan are shown in Fig. 5 for the situation where beam is extracted shortly (10 μs) after the end of 100 μs of accumulation. The scan provides a good measure of the beam distribution just after capture in the ring and before foil scattering can cause appreciable emittance growth. In Fig. 5 it is readily apparent that the beam distribution extends to about 38 mm, which corresponds to the value of the limiting aperture defined by the extraction septum. Note that

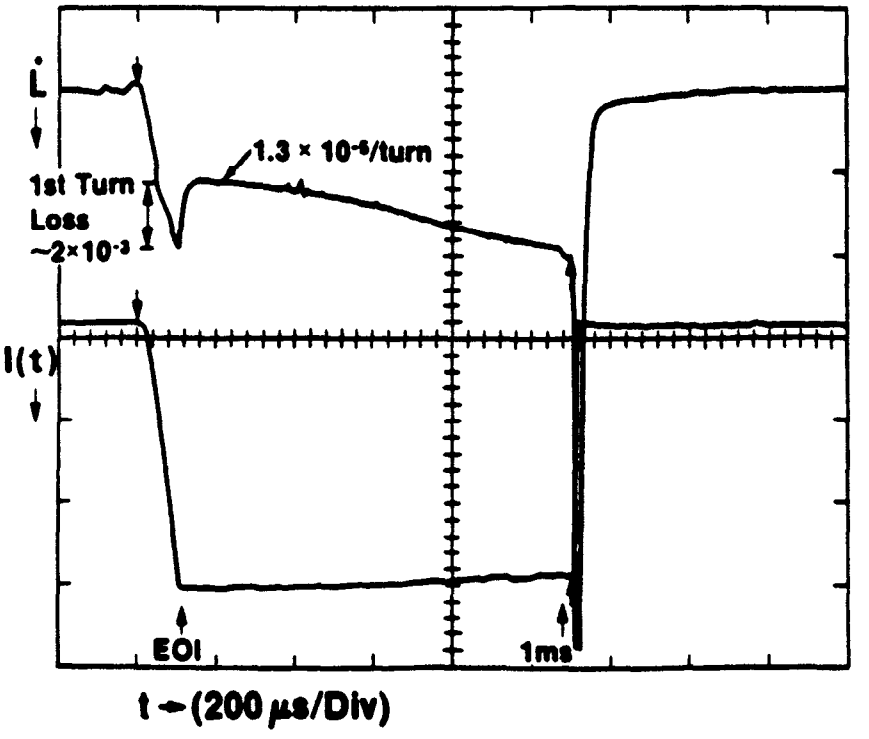

Fig. 4. Loss rate for 1 ms storage.

the beta functions at the septum and at the halo plate are nearly equal.

The mismatched Gaussian (MM GAUSS in Fig. 5), described in the next section, fits the distribution of Fig. 5 very well.

3.2. Emittance Growth and Losses During Injection

It may seem surprising that the beam fills the horizontal acceptance at injection since the acceptance of PSR, $\sim 130\pi$ mm-mrad, is so much larger than the rms emittance, $\sim 0.5\ \pi$ mm-mrad, of the H^- beam from LAMPF. The momentum spread (rms) of the H^- beam is also small with $\Delta p/p \simeq 5 \times 10^{-4}$. Two main factors contribute to emittance growth in the injection process: 1) an increase in horizontal divergence in the stripper magnet when H^- is converted to H° and 2) a large horizontal optics mismatch of the H° beam to the PSR acceptance.

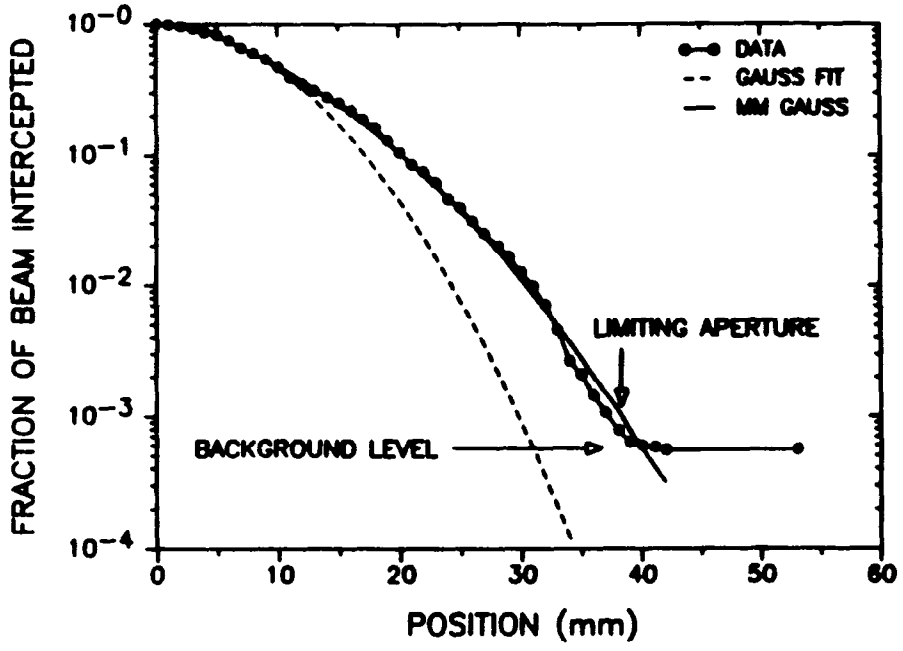

Fig. 5. Horizontal haloplate scan.

A Gaussian fits the core of the beam but fails to fit the extremities. Stripping of the H^- in a high magnetic field is a stochastic process which leads to random fluctuations in the point of conversion and thus an increase in H^o-beam divergence. Calculations of the angular distribution for a pencil beam of H^- are shown in Fig. 6 for two different vertical entrance positions (y = 0 at midplane and y = -4 mm). The calculation used the measured field map of the stripper magnet and a parameterization of the H^- lifetime from earlier Los Alamos work.[3] Emittance growth in the stripper magnet is minimized by use of a small gap magnet with a high field gradient at the entrance and by optics which produce a very small spot in both x and y at the stripper magnet. Even with this optimization the horizontal emittance of the H^o is three (3) times larger than that of the incoming H^- beam.

An optics mismatch at injection, shown in Fig. 7, is an additional consequence of magnetic stripping. The H^o is constrained to diverge from a small spot at the stripper magnet and cannot be matched simultaneously in the (X,X′) and (Y,Y′) planes at the standard location of the foil stripper where the H^o is reasonably well matched in (Y,Y′) but badly mismatched in the (X,X′) plane.

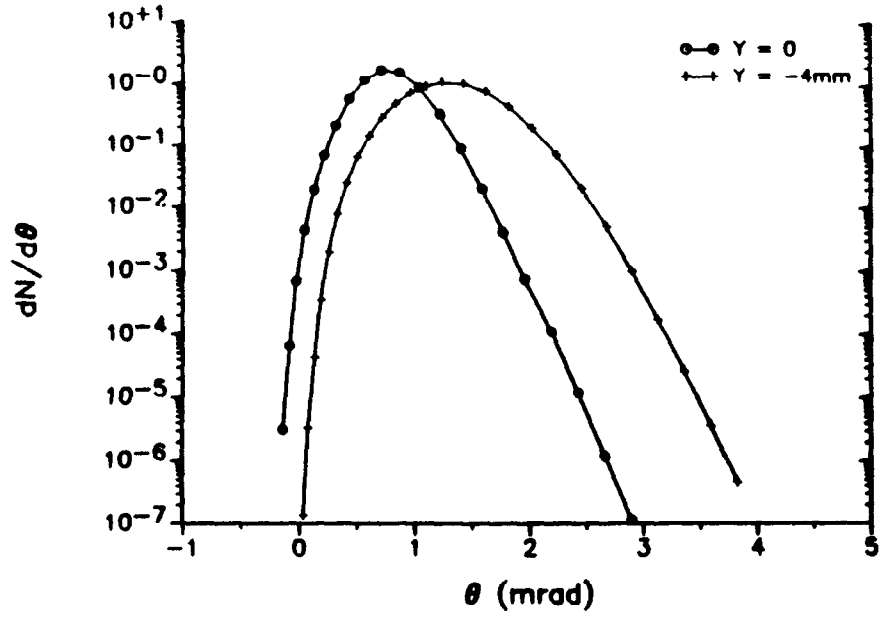

Fig. 6. H^o distribution after stripper magnet.

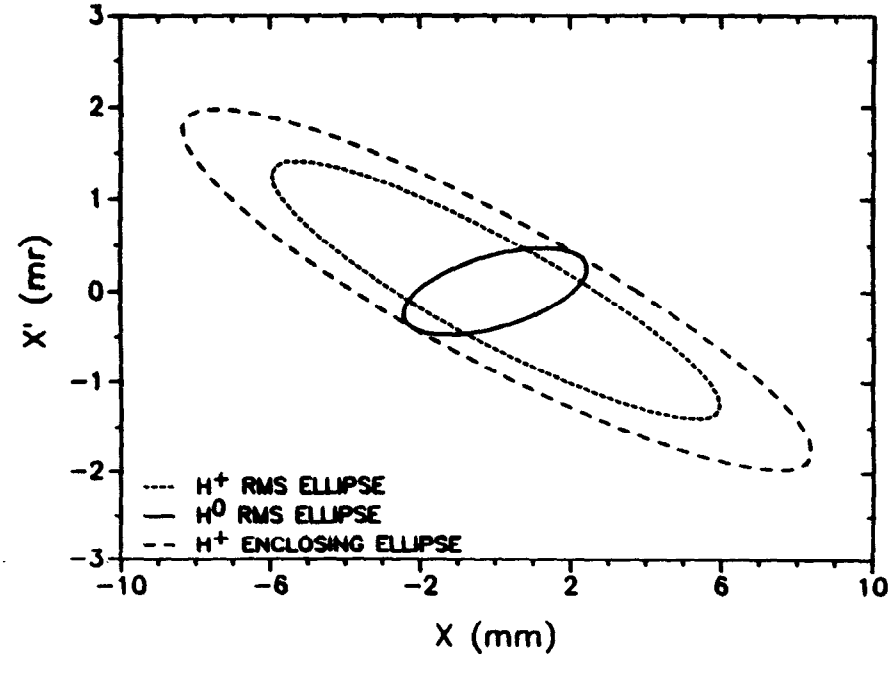

Fig. 7. Injection mismatch in horizontal plane.

The mismatch factor, $C = \{\beta_o\gamma_R + \beta_R\gamma_o - 2\alpha_o\alpha_R\}/2$, (subscript o refers to H° and R to the ring) has a value of 3.8 indicating a further increase of 3.8 in the rms emittance of the stored beam. The mismatch also changes the beam distribution; for a Gaussian beam injected on axis, one can easily obtain the following closed form for the distribution of the invariant betatron amplitude, y: $P(y)dy = \frac{1}{\epsilon_o}\, e^{\frac{-Cy^2}{2\epsilon_o}}\, I_o\left(\frac{y^2}{2\epsilon_o}\sqrt{C^2-1}\right)\, y\, dy$ where ϵ_o is the rms emittance of the incoming H° beam and I_o is a modified Bessel Function.[4] The rms emittance for this distribution is $C\epsilon_o$. This distribution has longer "tails" than a Gaussian with the same rms emittance, thereby increasing still further the size of the beam near the limiting apertures. The non-Gaussian tails are readily apparent at PSR in the halo-plate scan shown in Fig. 5 and in wire-scanner profiles of the extracted beam taken at the end of short (100 μs) accumulation as shown in Fig. 8. The "mismatched" Gaussian distribution derived from equation (1) fits the data very well whereas a Gaussian with the same rms width fits poorly, especially at large X.

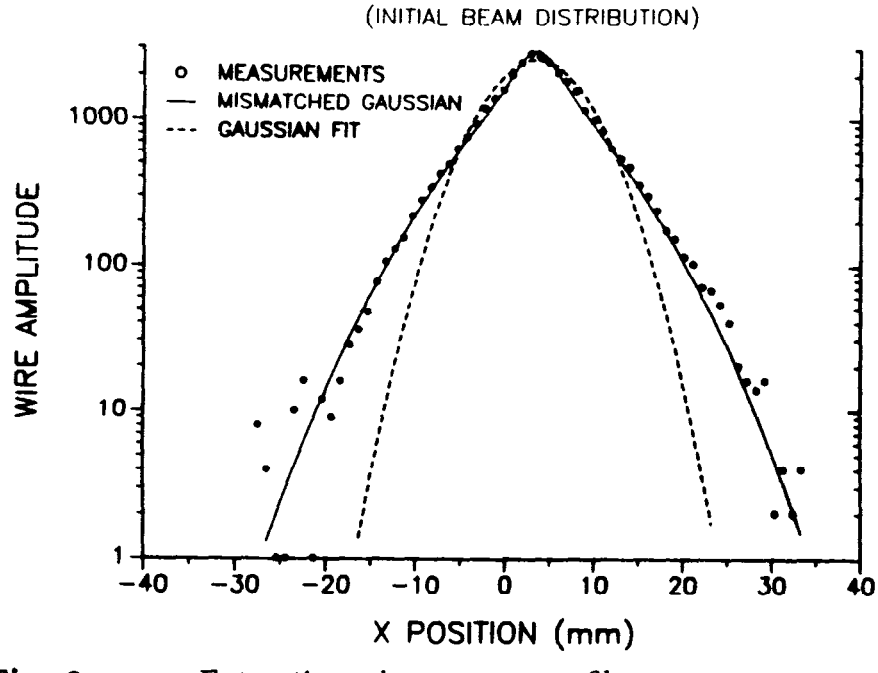

Fig. 8. Extraction wire-scanner profile.

Integration of the distribution described by equation (1) for the region outside of the limiting aperture provides an estimate of injection or "first-turn" losses. A value of 2 to 4 x 10^{-3} is obtained which is in good agreement with the observed value of $\sim$ 2 x 10^{-3} considering the high sensitivity of the result to the size of the limiting aperture.

3.3 Emittance Growth and Losses During Storage

A typical proton in PSR traverses the injection foil during about half of its revolutions. Multiple Coulomb scattering in the foil will cause emittance growth (rms) given by $\epsilon(t) = \epsilon_o + \beta_f \theta_1^2 f N(t)/2$ where ϵ_o is the initial rms emittance, β_f the beta function at the foil, θ_1 the rms scattering angle from a single foil traversal and fN(t) the number of foil traversals in N turns up to time t. The rms emittance is defined as $\sqrt{<X^2><\theta^2> - <X\theta>^2}$ where <> indicates expectation value and $\theta = X'$. Measurements of beam sizes as a function of storage time shown in Fig. 9 are well fit by the above equation for $\epsilon(t)$ and show nearly a factor of three increase of emittance (proportional to square of the spot size) during 1 ms of storage.

To accurately estimate losses from multiple Coulomb scattering requires more than knowledge of the rms emittance growth; one must calculate the evolution of the distribution function with time. We have made estimates using two different methods which produce similar results in reasonable agreement with measurements. The first method used a Fokker-Planck equation

$$\frac{1}{K}\frac{\partial P}{\partial t}(t,y) = \frac{\partial}{\partial y}\left[y \frac{\partial}{\partial y}\left(\frac{P(y)}{y}\right)\right] \qquad (2)$$

which was derived for estimating beam lifetimes in the presence of Coulomb scattering by residual gases.[5] Here y is the invariant betatron amplitude and K a constant. Solutions for the distribution function, P, are obtained as a Fourier-Bessel series and integrated to obtain the losses.

Similar results are obtained with the Monte Carlo tracking code, ARCHSIM, developed for modeling circular machines.[6] The tracking code simulates emittance growth in the stripper magnet and treats scattering in the stripper foil as a combination of multiple Coulomb scattering with single Coulomb and nuclear tails.

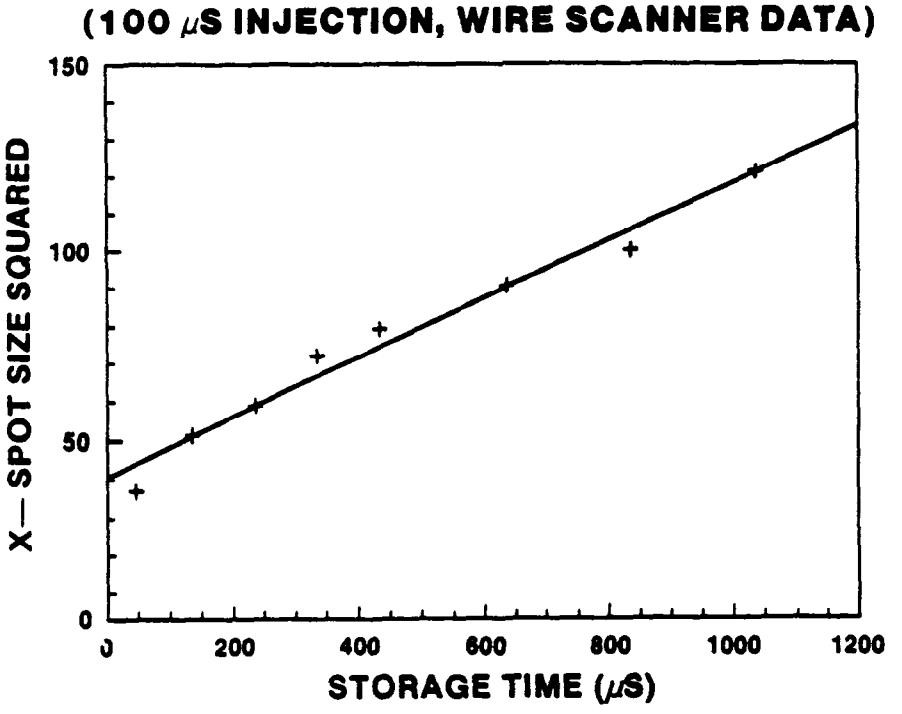

Fig. 9. Emittance as a function of storage time.

Results from the simulation and from solutions of the Fokker-Planck equation made using measured values of parameters in the models are compared in Fig. 10 with measured data on loss rates. The loss rates obtained using solutions of equation (2) were augmented with a constant term which takes account of nuclear scattering and large-angle single Coulomb scattering. Agreement between calculations and measurements are within the calibration uncertainties of the losses and the errors on parameters in the calculations. Losses are sensitive to several parameters including the mismatch factor, the H° distribution, the probability for traversing the foil, and to the size of the limiting aperture. With small adjustments of parameters, within errors, both calculations can be made to agree completely with the loss-rate data.

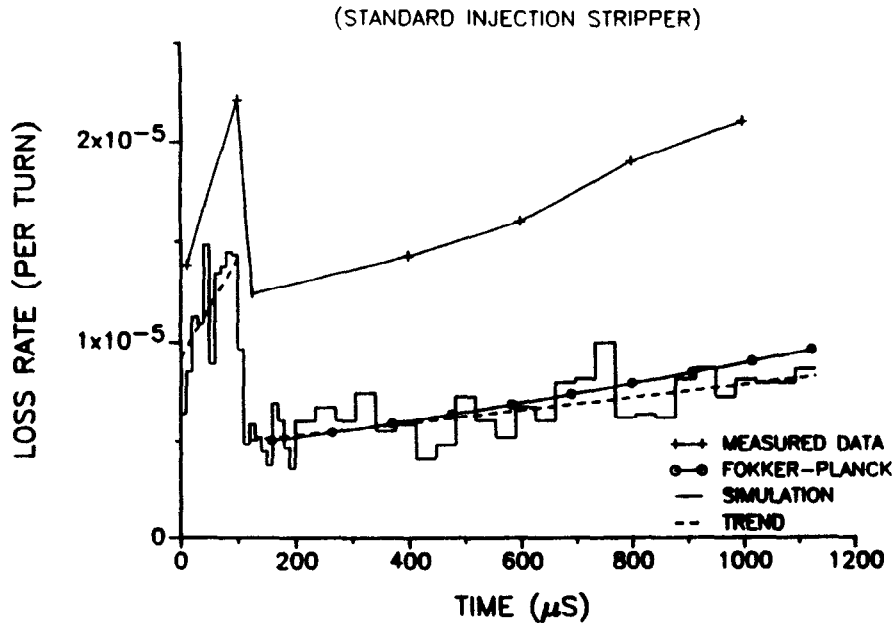

Fig. 10. Loss-rate calculations and measurements.

3.4 Effect of the RF Buncher

An RF buncher is used to maintain an empty gap to accommodate the extraction-kicker rise time. Synchrotron motion induced by the buncher increases the momentum spread to ~0.3%; because of dispersion the beam size increases by several mm and also contributes to beam losses. For long storage, this shows up as a striking modulation of the loss rate with a frequency twice that of the synchrotron oscillations as shown in Fig. 11. Losses are increased by about 45% when the RF is on at typical operating set points.

3.5 Other Contributions

Losses from nuclear scattering are readily estimated from the total cross section as 3.3 x 10^{-6} per foil traversal. The contribution from large-angle single Coulomb scattering is often overlooked. Because the cross section falls off only as a power law, rather than as an exponential, it contributes a long tail to any beam distribution. This was seen at PSR when the injection foil location was

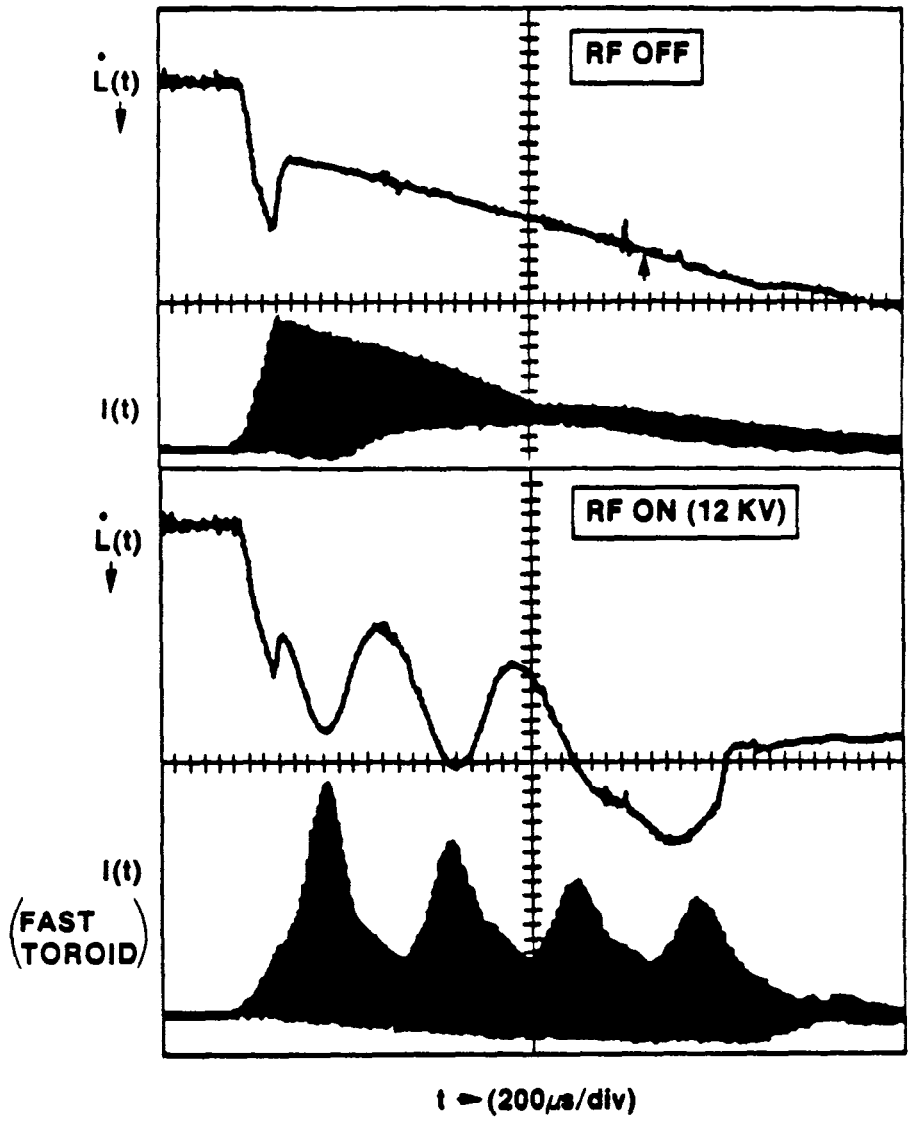

Fig. 11. Effect of RF buncher on loss rate.

changed to provide a better match in the (X,X′) plane. The halo-plate scan of the beam distribution (after a short accumulation) plotted in Fig. 12 shows the expected reduction in size of the core of the beam. Also seen is a tail extending to the limiting aperture. The size and shape of the tail agrees with analytical and Monte Carlo calculations of the contribution from single Coulomb

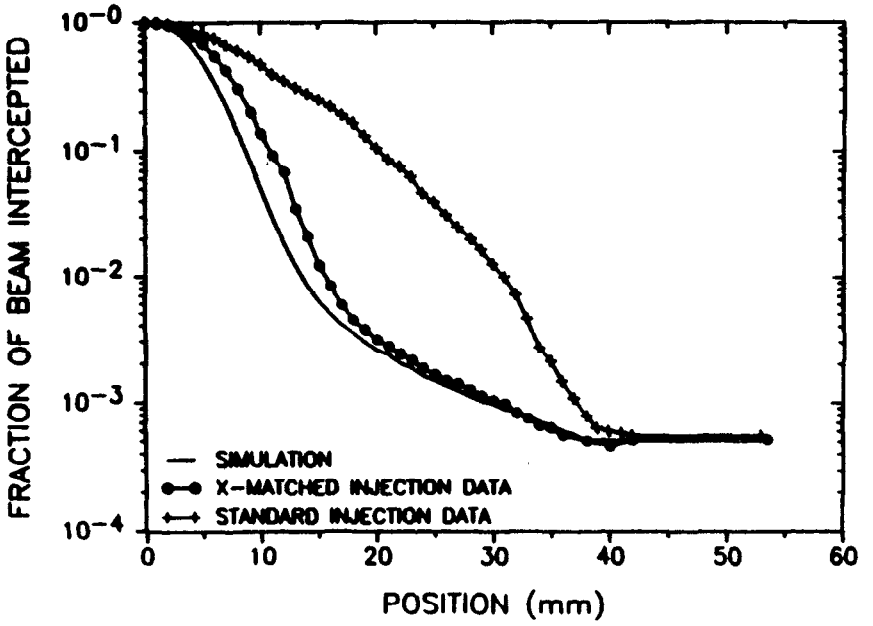

Fig. 12. Evidence for single Coulomb scattering.

scattering. At PSR large-angle Coulomb scattering contributes a loss rate of $\sim 2 \times 10^{-6}$ per foil traversal for a δ function initial distribution and more for a beam of finite emittance.

3.6 Summary of Losses During Accumulation

The composition of accumulation losses during standard operation of PSR (375 μs injection period) can be determined from the data and analysis presented here. Results are listed below:

"First-Turn"	0.2%
Nuclear and Large-Angle Coulomb Scattering	0.2%
Emittance Growth in Absence of RF	0.6%
Effect of RF	0.5%
Total	1.5%

4. Upgrade of PSR to Reach 100μA

Increasing the operating current of PSR is a high priority goal for the Los Alamos National Laboratory. Management is committed to providing the upgrades needed to reach 100μA with beam avail-

ability of 75% or more. Our present understanding of the causes and mechanisms of the slow losses has pointed to several promising measures for significantly reducing or controlling the losses in the PSR. These are sketched below.

4.1. Ring Halo Collimation System

Initial design studies assumed that a collimation system would be used to control the location of losses in the ring but none were designed or implemented in the initial construction. Plans for experimental study of the problem last summer were preempted by the more urgent need to improve reliability. The basic idea is to make scrapers or collimators the limiting apertures of the ring in such a way that the losses are moved from a critical component, such as the extraction septum, which is the present limiting aperture, to passive absorbers that are designed to deal with higher activation. These would be passive devices which would not need frequent service and would be located in less congested areas where activated components are more easily dealt with.

The two basic concepts are illustrated in Fig. 13a and b. In one (a) a high Z, movable scraper, such as 10 mm of tungsten, intercepts the beam halo and defines the limiting aperture. It is not thick enough to completely absorb the incident beam but scatters it by a relatively large amount so that most of the intercepted beam is caught by the downstream thick absorber, which is not a limiting aperture. A small fraction (perhaps 10%) of the intercepted and scattered beam goes through the opening of the absorber and is caught on a "cleanup" absorber or is lost elsewhere in the ring. If much of the beam intercepted by the scraper is beam that would have been lost elsewhere, such as at the extraction septum, then this system would be effective in reducing the losses elsewhere in the ring.

In the second concept (Fig. 13b), a moveable absorber also intercepts the beam halo and defines the limiting aperture. It is thick enough to absorb most of the incident beam. The difficulty with this concept is the "slit scattering" which occurs from the large surface of the moveable absorber struck by beam particles at grazing incidence. The amount of scattering and the fraction of

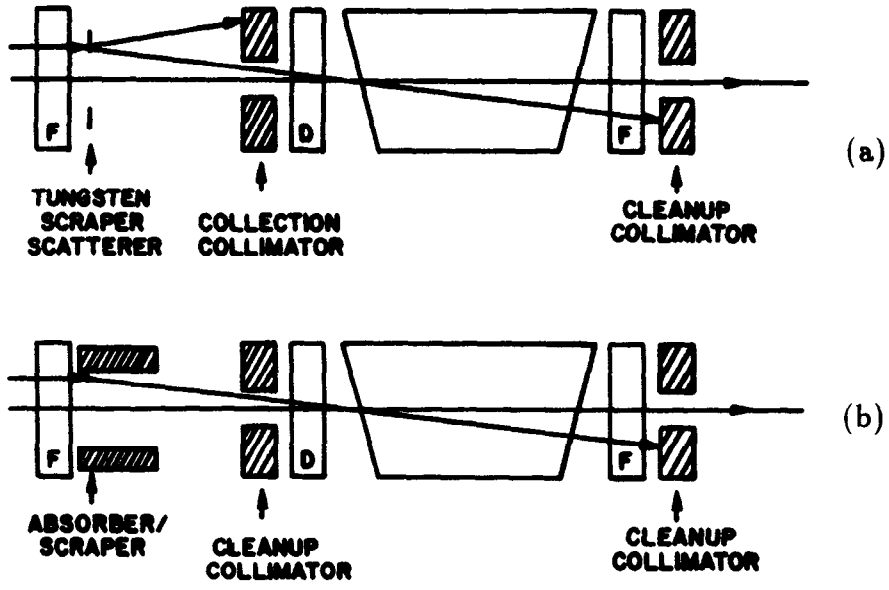

Fig. 13. Halo collimation concepts.

the scattered beam that spills elsewhere in the ring are not easily estimated.

More detailed study of these options is needed to determine which is best for PSR. Performance of the first option is more readily estimated. It has the advantage that the large scattering angles spread out the heat load on the absorber such that it may not need water cooling. The small moving scraper is a simpler mechanical device that is lightweight and probably does not need water cooling. Depending upon the amount of slit scattering, the second option may be more the efficient one in localizing the losses. However, it does have some disadvantages; the heat load is concentrated near the inner surface of the moveable absorber and it may well need water cooling. A large, moveable, water-cooled absorber is a complicated mechanical system that may require more frequent servicing, thus compromising the goal of containing the activation in highly reliable, passive devices that would seldom need servicing or removal.

4.2. Options for Improved Injection

It is now clearly understood that the key to reducing losses is reducing the number of times a stored proton traverses the stripping foil. In the present operation the probability for a stored beam particle to traverse the foil is between 50 to 100% per turn. A major goal for the upgrade is reducing this to around 5% or less primarily by improving the injected beam tune (some times called "match" or "matching"), improving injection "painting" in transverse phase space, and increasing the horizontal aperture of the ring.

4.2.1. Improved Painting in Phase Space

Injection "Painting" refers to procedures such as fixed offsets or programmed bumps used to control the beam density or other aspects of the way injected beam fills the phase-space acceptance of a ring. It can be used to reduce the number of foil traversals by the stored beam.

A fixed offset allows betatron motion to fill an interior region of phase space. A fixed vertical offset, which is depicted in Fig. 14, is presently in use at PSR. It was intended that the edge of the foil be on the vertical closed orbit of the ring and two standard deviations below the center of the H^o beam. This should result in a 50% probability per turn for the stored beam to intercept the foil. At PSR we have had, in the past, a good deal of uncertainty regarding the parameters of the H^o beam at the foil and thus the probability for the stored beam to hit the foil. With improved diagnostics and improved analysis procedures, we expected to resolve this issue in the coming running period.

A programmed closed-orbit bump is essentially a way to introduce an offset that varies with time. It can be used to move the stored beam off the foil so that some of it will not be able to hit the foil thereafter. The time profile of the bump can be chosen to optimize the beam spatial distribution or the foil hitting probability. For a given acceptance, the use of optimized programmed bumps improves both the beam density distribution and the foil-hitting probability compared with a fixed offset.

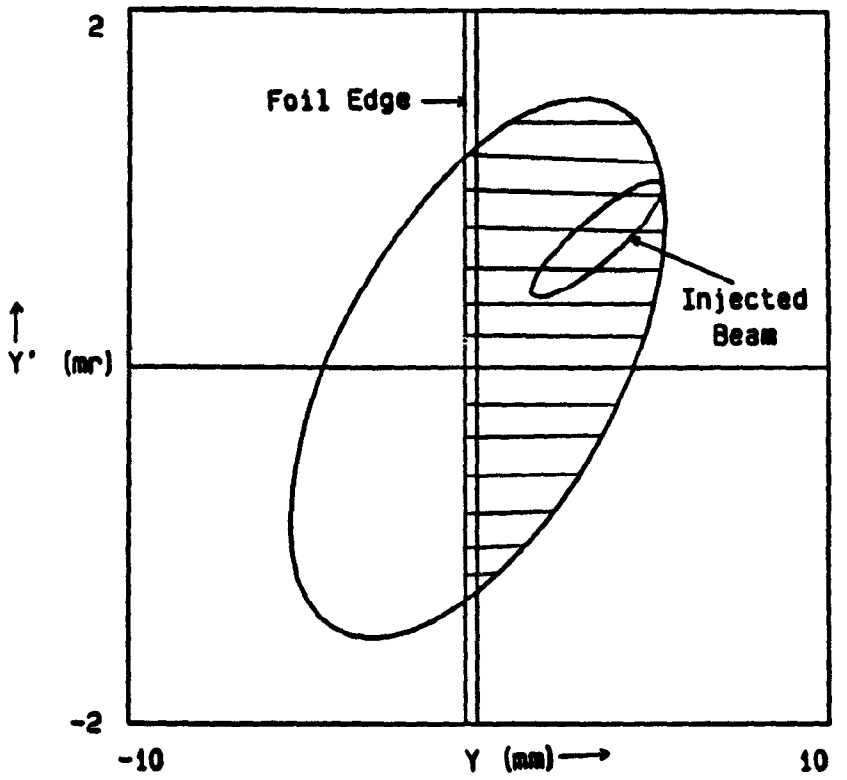

Fig. 14. Standard H^o injection at PSR with vertical offset.

4.2.2. Improved Injected-Beam Tune

From an examination of Fig. 14, it is obvious that the foil hitting probability can be reduced by changing the shape and orientation of the H^o ellipse. Without changing the area of either the H^o or H^+ beam ellipses, and while changing only the shape to a narrower, upright ellipse, the foil-hitting probability can be reduced by a significant factor ($\sim$4) as illustrated in Fig. 15. Unfortunately, such a tune of the H^o beam cannot be achieved with our system for generating H^o, given the location of the stripper magnet and the injection foil.

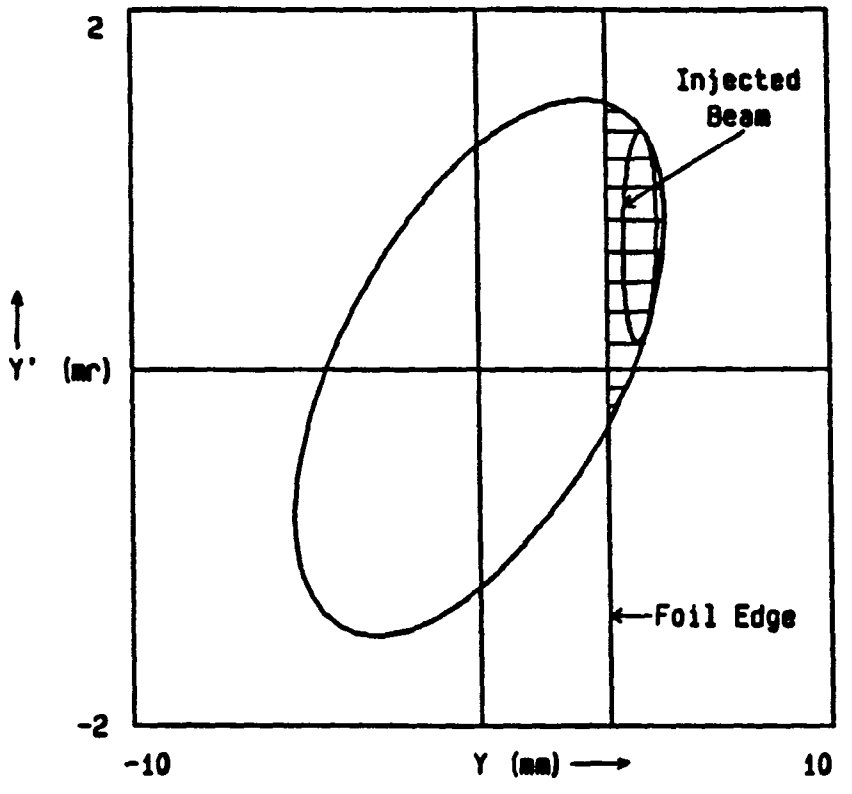

Fig. 15. Offset injection with the H^o tune optimized to reduce foil traversals by the stored beam.

4.2.3. Improved Injection Foils

The carbon foils presently used at PSR are mounted on a C-shaped frame that supports the foil on three sides leaving a horizontal edge unsupported. The foil is positioned vertically to cover all of the vertically offset H^o beam but not all of the stored H^+ beam. Thus, the foil covers the full horizontal aperture of the ring while in the vertical it covers less than the full aperture. An ideal foil for reducing losses would have a massless support with stripping material only in the region of the H^o beam spot.

A number of suggestions have been made for improving the foil support in ways that should reduce the probability for the stored beam to hit the foil. Yamane[7] at KEK has proposed "corner" foils for the JHF Compressor/Stretcher Ring. His foils have two unsup-

ported edges and can be positioned to cover an H^o beam offset in both dimensions while intercepting less of the stored beam. He has successfully tested corner foils with a low-energy nitrogen beam. This is a promising development for PSR and we will collaborate with KEK on tests of corner foils and other improvements to H^o injection.

Another concept being investigated at PSR is the use of very fine carbon filaments (4- to 5-microns diameter) to support carbon foils. This is work carried out in collaboration with a team from Westinghouse who have facilities at Hanford, Washington to fabricate foils supported in this manner. We expect to test fiber-supported foils in the beam during the 1989 running period.

4.2.4. Improved H^o Injection

The present method of injection using H^o can be improved using the techniques described above. However, it is much more difficult to improve the H^o beam tune at the foil since it is not possible to focus a neutral beam. One can only manipulate the H^- beam before it is converted to H^o or change the ring lattice so that the H^+ beam (ring ellipse) better "matches" the fixed H^o beam. The constraints at the stripper magnet with its small gap severely limit the tuning of H^-. One can improve the match of H^o to the ring by moving the stripper foil to a location just upstream of the focusing quadrupole. Rotation of the stripper magnet, as proposed by Yamane,[7] can also help.

The important question is whether H^o injection can be improved sufficiently to meet our goal of reducing losses by an order of magnitude. We expect to answer this question with further analysis and experiment this summer.

4.2.5. Direct H^- Injection

H^o injection suffers from two disadvantages: (a) the growth of emittance (about a factor of 3 for PSR) in the bend plane of the stripper magnet and (b) lack of flexibility in tuning the beam for optimum beam parameters at the injection foil. A way around

both of these difficulties is to inject the H^- beam directly. A scheme for doing this at PSR is shown in Figs. 16 and 17. The current in the two ring dipoles on either side of the injection straight section is reduced about 10% so that each bends the protons 3° less. The closed orbit of the stored beam is restored by the addition of a low-field dipole which bends protons by 6°. The field of this dipole is about 3.8 kG, which is low enough to cause negligible stripping of the H^- beam. An H^- beam can be transported to enter the low-field dipole in such a way that the H^- emerges from the dipole on top of and aligned with the stored H^+ beam. A stripper foil to convert H^- to H^+ follows. Some H^o will emerge

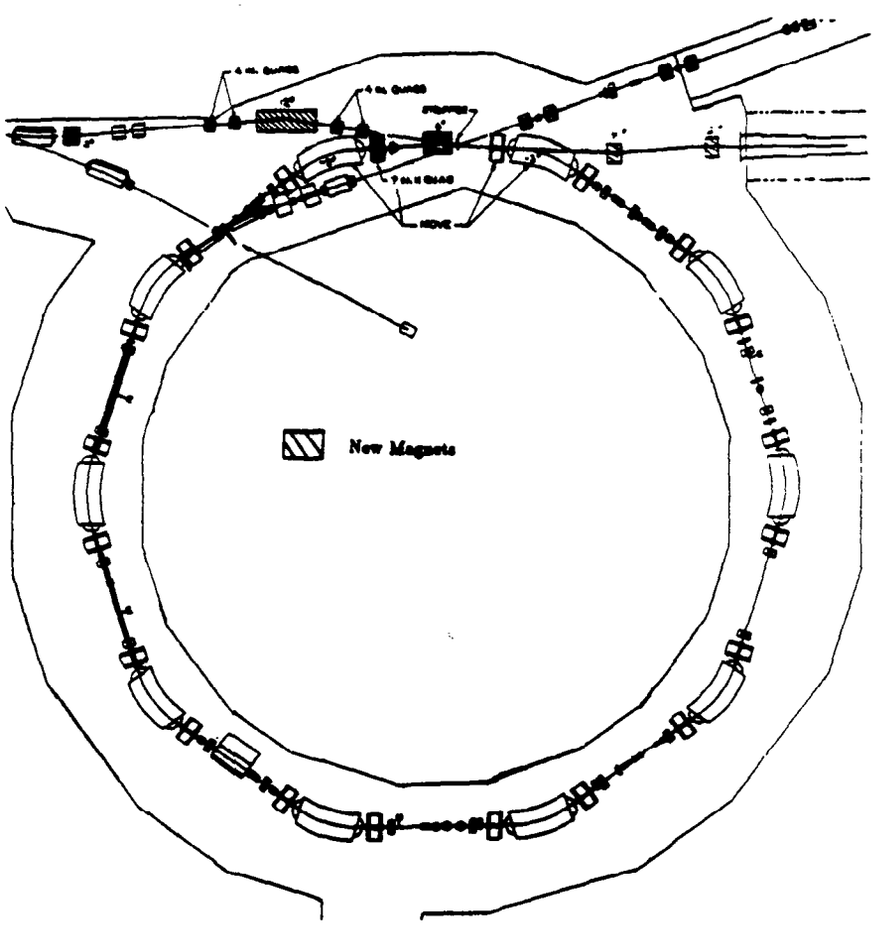

Fig. 16. Layout of PSR with direct H^- injection.

from the stripper foil; in addition, some H^- will miss the foil and be stripped to H^o in the fringe field of the ring dipole. Provisions are made to transport both H^o beams to the existing H^o beam dump.

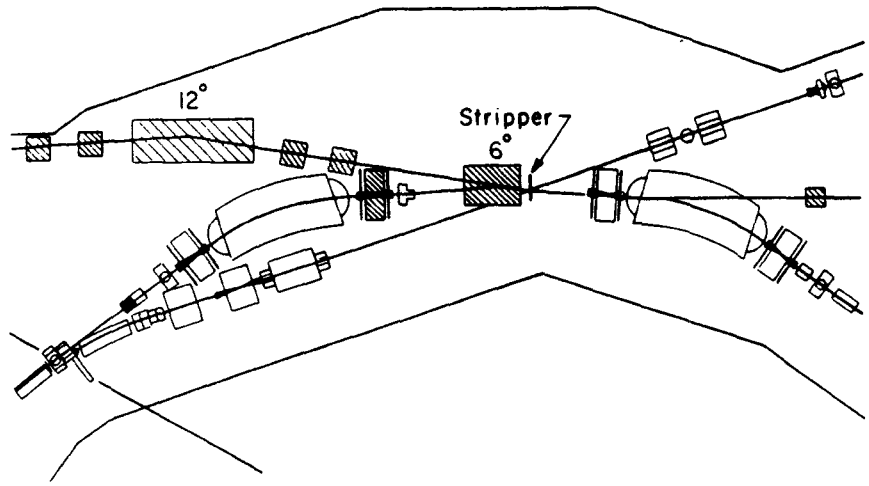

Fig. 17. Injection region for direct H^- injection.

Design studies are underway to find the optimum injection parameters for direct H^- injection and to estimate the improvement expected with respect to beam losses. Our planning for the upgrade assumes direct H^- injection since it offers greater promise for the needed reduction in losses. However, if it can be shown that the needed improvement is possible with less costly modifications of the H^o injection, then we would proceed in that direction. More study is needed before a final decision is made.

4.3. Increased Aperture

Much of the beam loss occurs at the extraction septum, which is the limiting aperture in the horizontal plane. The rest of the ring has considerably more aperture; both the quadrupoles and the dipoles have larger horizontal apertures. The septum is a limit because the present extraction kickers are unable to provide a larger kick. A 50% larger kick (about 18 mrad) would allow the septum to be placed further from the stored beam and thereby increase the aperture by 50% and result in a factor of two larger acceptance of the ring in the horizontal phase plane.

Options which would provide the larger kick needed for full aperture extraction are under study. R & D on a ferrite kicker system is underway; a prototype pulser has been designed and is being fabricated at SAIC. The goal is a ferrite kicker system which provides 18 mrad of kick from ferrite magnets which occupy only one section of the ring instead of two. With the larger kick one may also need to replace the dipole and quadrupole just downstream of the kicker with ones of larger aperture to insure that the extracted beam is not distorted by nonlinear fields.

The larger aperture has two main advantages. The increased acceptance can be used to make painting more effective in keeping the beam off the foil for either H^o injection or direct H^- injection schemes. In the process of using the increased aperture to improve painting, the horizontal beam size will increase thereby reducing beam density and associated space-charge effects.

4.4. Other Means of Reducing Losses

Other methods to reduce losses include increasing the H^- beam intensity from the linac and/or increasing beam brightness by reducing emittance and beam halos. Increased intensity will reduce losses by reducing the accumulation time, hence, the number of foil traversals needed to achieve a given average current from the ring. Reduced emittance increases the effectiveness of all injection painting methods in keeping the stored beam off the injection foil.

Some efforts are underway to develop a higher intensity H^- source. These are not considered part of the present upgrade, but, as longer range studies aimed at longer-range improvements. If additional reduction in losses is needed for the upgrade, these efforts might be accelerated.

4.5. Improved Beam Diagnostics

Good beam-diagnostic instrumentation is necessary for a variety of reasons. Reliable, accurate, and well-understood instruments are needed for precise control of high-intensity beams and for conducting an efficient operation. They are also essential tools for effective experimental studies of beam dynamics issues. The present beam-position monitor (BPM) system needs improvement; it is sensitive to only the 201-MHz component of the beam. This is suitable

for use in the transport lines from the linac and for sensing the freshly injected beam at PSR, but not for locating the stored beam in the ring or in the extraction line. The present BPM's are also of limited use for studying broad-band phenomena such as the transverse instability. A program of BPM development is underway to develop instruments that satisfy these needs.

Knowledge of the distribution of H^- beam in transverse phase space is needed for careful setup of injection conditions. Present methods of reconstructing only the rms emittance are proving to be major limitations to a good optimization of injection parameters. It is likely that a slit and collector method will need to be implemented to directly measure the phase-space distributions.

4.6. Role of the Transverse Instability

A coherent transverse instability has been seen at higher peak intensities at PSR. It is described in more detail elsewhere.[8] It is generally believed that we can run at 3 x 10^{13}ppp without the need for new hardware, such as an active damper, to control the instability. Some experimental studies have shown more or less stable operation at up to 4 x 10^{13}ppp using existing hardware to control the instability primarily by Landau damping. The techniques to enhance Landau damping, such as use of sextupoles and octupoles, generally increase the slow losses. In planning for the upgrade we assume that the instability is under control with the present hardware. However, more detailed experience with high peak currents is warranted and may change the present perception of the importance of the instability to the 100-μA goal.

4.7. Goals and Status of the Upgrade

The goals of the upgrade are to develop and implement changes to PSR which will result in reliable delivery of 100μA at 20 Hz with beam availability greater than 75%. It is also a goal to complete the upgrade over the next three years and have it commissioned by the end of 1991. The planning for the upgrade is at the stage where numerous options are still being studied and R&D work on certain issues is underway. The scope of the project is known but much work remains before all choices are finalized. A conservative plan would include collimation in the ring, direct H^- injection,

increased aperture, and improved diagnostics carried as far as the present technologies permit. Budget realities cause us to seek the most cost-effective solution which meets our goals.

5. Perspective on the Storage Ring Option

Enough experience has been gathered from PSR to offer some perspective on the storage- or compressor-ring option as the driver for an advanced neutron source. One must be careful to separate the generally applicable features of the experience from those which are due to local factors that are not particularly relevant elsewhere.

5.1. Reliability

Poor reliability has become a stronger issue at PSR than it should be in general for a dc storage ring. It reflects past budget constraints coupled with changing requirements for the ring. The so called "short-burst mode" was the technically more challenging problem that drove many choices. That mode was discontinued late in the construction after numerous choices had been made. There was not an opportunity to redo the optimization for the needs of the long-burst mode.

Good reliability was never an articulated, high-priority design goal for the PSR. It was and is too easy to compromise reliability to reduce initial construction costs. To some extent this will always happen but if reliability is a high-priority goal it should be included in the basic design goals.

5.2. Losses

Losses are a difficult technical problem for most high-intensity proton machines. There is a not a well-established theory for dealing with losses. Apart from the meson factories, there is not much experience to draw on. From the PSR experience, we can say that losses can be understood; but it requires careful, detailed work. We can also say that losses cannot be ignored; they, too, must be treated as a fundamental requirement in the design.

5.3. H^o Injection

With the benefit of hindsight, we would not recommend H^o injection for a high-intensity accumulator or compressor ring. We do

not imply that H^o injection cannot work, but rather, that direct H^- injection is better. It does not suffer the significant emittance growth inherent in the use of magnetic stripping and a charged beam is much more easily manipulated to meet the various requirements for an optimized tune at the stripper foil.

5.4. Conclusions

While there have been disappointments in the experience with PSR, they do not discredit the compressor-ring option as a driver for an advanced spallation neutron source. Compared to a ring that must accelerate as well as accumulate, the storage ring is intrinsically simpler. The one drawback is that injection losses in a storage ring, such as PSR, occur at the full energy rather than at a lower energy as is the case for a rapid cycling synchrotron typified by ISIS. One can tolerate and handle larger losses at lower energy.

There are several promising options for reducing or controlling losses at PSR. We are confident that a subset of these will enable PSR to reach 100μA at 20 Hz. We expect to report operation with enhanced reliability and good beam availability in 1989 and increasing currents thereafter.

Acknowledgements

This work was performed under the auspices of the U. S. Department of Energy.

References

1. G. Lawrence, "The Performance of the Los Alamos Proton Storage Ring," Proc 1987 IEEE Particle Accelerator Conference, pp. 825-829.
2. R. Macek, D. H. Fitzgerald, R. L. Hutson, M. A. Plum, and H. A. Thiessen, "Analysis of Beam Losses at PSR," Proceedings European Particle Accelerator Conference, Rome, June 7-11, 1988. To be published
3. A. Jason, D. Hudgins, and O. van Dyck, "Neutralization of H− Beams by Magnetic Stripping," IEEE Trans. Nucl. Sci., NS-28, pp. 2704-2706 (1981).

4. R. Macek, "PSR Beam Distributions II: Mismatched Gaussian," Los Alamos National Laboratory PSR Technical Note #153, October 1987.
5. H. Bruck, "Circular Particle Accelerators," LA-TR-72-10 Rev., Chap XIV (1972). Translation from French original "Accélérateur Circulaires de Particules" (1966).
6. H. A. Thiessen, "ARCHSIM Primer," Los Alamos National Laboratory, PSR Technical Note 89-002, March 1989.
7. I. Yamane, K. Kitagawa, H. Someya, and Y. Yano, "Injection of 1 GeV H^- Beam into the JHF I-A Ring," KEK Report 88-8, November 1988. Also I. Yamane, "JHP Compressor/Stretcher Ring and Its Injection Scheme," invided talk at 1989 AHF Accelerator Design Workshop, Los Alamos, February 20-25, 1989, KEK Preprint 88-121, January 1989.
8. D. Neuffer, E. Colton, G. Swain, H. Thiessen, B. Blind, R. Hardekopf, A. Jason, G. Lawrence, R. Shafer, T. Hardek, J. Hurd, and R. Macek, "Transverse Collective Instability in the PSR," Particle Accelerators, 1988, Vol 23, pp 133-148.